Soil property-based methods for design of nondisplacement piles

R. Salgado
Professor, School of Civil Engineering, Purdue University, West Lafayette, Indiana, USA
M. Prezzi
Professor, School of Civil Engineering, Purdue University, West Lafayette, Indiana, USA
F. S. Tehrani
PhD Student, School of Civil Engineering, Purdue University, West Lafayette, Indiana, USA

2011 Pan-Am CGS Geotechnical Conference

ABSTRACT
Recent research has produced soil property design methods for calculation of the ultimate load capacity of nondisplacement piles (drilled shafts) based on results of advanced analyses using realistic constitutive models. This paper discusses important aspects of these analyses and their results for both shaft and base resistance of nondisplacement piles installed in sand and clay. The design equations that resulted from these analyses can be used to calculate the unit shaft resistance and the unit base resistance of nondisplacement piles installed in clay and in sand. Predictions using the proposed equations compare well with the data obtained from several field pile load tests.

RÉSUMÉ
Au cours de la dernière décennie, la recherche a produit des méthodes de calcul de la capacité de charge de rupture à partir des propriétés du sol basées sur des analyses de haute qualité, en utilisant des modèles réalistes constitutive. Cet article examine les analyses et leurs résultats pour la résistance de base et de l'arbre de pieux nondisplacement (foré puits) installés dans le sable et d'argile. Sur la base de ces simulations, il est possible de proposer des équations pour la friction de l'axe coefficient qui peut être utilisé dans le calcul de la résistance du fût de puits forés dans l'argile et de la contrainte normale effective sur le fût du pieu qui peut être utilisé dans le calcul de la résistance du fût dans le sable, ainsi que les équations de base pour la résistance dans le sable et d'argile. Les prévisions en utilisant les équations proposées se comparent bien avec les données issues de différents essais sur le terrain de chargement de pieux. Il est soutenu que la conception de pieux dans le futur sera de plus en plus fondée sur les résultats scientifiques.

1 INTRODUCTION

Piles are often used as foundations of various types of structures. There have been significant developments in pile installation techniques and piling technology in the last few decades. However, development of methods of analysis and design for piles has lagged behind. This is primarily due to the fact that rigorous analysis of pile installation and loading is very complex. Given the complexities involved, design methods have been based mainly on empirical approaches.

Over the last decade, as a result of advancements in computational methods and in methods of analyzing geotechnical boundary value problems, soil property-based methods of calculation of the ultimate load capacity of nondisplacement piles have been proposed. These design methods are based on the results of advanced analyses using realistic soil models. In this paper, we discuss these analyses and how their results can be used in the calculation of both unit base and unit shaft resistance of nondisplacement piles installed in sand and clay.

2 PILE CAPACITY

The total load that is carried by a pile can be expressed as the sum of the ultimate load $Q_{b,ult}$ carried at the pile base and the limit load Q_{sL} carried by the pile shaft (Salgado 2008):

$$Q_{ult} = Q_{b,ult} + Q_{sL} = A_b q_{b,ult} + \sum_{i=1}^{i=N} A_{si} q_{sLi} \qquad [1]$$

where $q_{b,ult}$ is the ultimate unit base resistance, q_{sLi} is the limit unit shaft resistance corresponding to the i^{th} soil layer along the pile length, A_b is the area of the base of the pile, A_{si} is the lateral surface area of the pile corresponding to the i^{th} soil layer, and N is the number of soil layers crossed by the pile.

As only small pile displacements (of the order of 0.25 – 1 % of the pile diameter) are required for complete mobilization of the unit shaft resistance, the unit shaft resistance is fully mobilized along a considerable portion of the pile length when the allowable axial load is applied

to the head of a well-designed end-bearing pile. The value of $q_{b,ult}$ calculated using a given method produces a value that is consistent with the criterion used to define $Q_{b,ult}$ in that method (e.g., for the 10%-relative-settlement criterion, $Q_{b,ult}$ corresponds to the load for which the pile displacement is equal to 10% of the pile diameter).

The ultimate load is that associated with the most critical ultimate limit state. An ultimate limit state (ULS) is a state at which the supported structure is unsafe: structural damage or collapse are associated with the concept of an ULS. Plunging of a pile is an ultimate limit state, but for most types of superstructure, the superstructure experiences severe damage at settlement levels much lower than that at which plunging starts. A common approach is to define ultimate limit states in terms of a limiting settlement, often expressed as a fraction (e.g., 10%) of the pile diameter.

3 PURDUE SAND METHOD FOR NONDISPLACEMENT PILES

Over the past decade, researchers at Purdue University have developed design methods based on rigorous analyses of nondisplacement piles (more specifically, bored piles or drilled shafts) in sand (Lee and Salgado 1999, Loukidis and Salgado 2008, Salgado and Prezzi 2007, Salgado 2008) that realistically simulate the load-transfer mechanisms along the pile shaft and at the pile base. We will now review these approaches.

3.1 Unit Shaft Resistance

The unit shaft resistance q_{sL} in sand is often determined using the β method, according to which:

$$q_{sL} = (K \tan\delta)\sigma'_v = \beta\sigma'_v \quad [2]$$

where, σ'_v is the *in situ* vertical effective stress at the depth at which q_{sL} is calculated, K is the coefficient of lateral earth pressure and δ is the interface friction angle mobilized at the pile-soil interface. Different methods can be used to estimate β (Reese et al. 1976, Stas and Kulhawy 1984, O'Neill and Reese 1999). However, most of the empirically-based methods are not valid for all sand types and do not always produce reliable estimates of β (O'Neill and Hassan 1994, Loukidis et al. 2008).

Loukidis and Salgado (2008) performed finite element analysis with an advanced constitutive model to investigate the load transfer mechanisms of nondisplacement piles in sands. They used an advanced, two-surface-plasticity constitutive model (see Loukidis and Salgado 2009) to simulate the response of the sand to loading. The constitutive model is capable of predicting the sand response in both the small- and the large-strain range, while taking into account the effects of the intermediate principal effective stress and of the inherent anisotropy of the sand. Finite element analyses of shearing along the pile shaft were performed in order to examine the changes in stress state around the shaft upon axial loading of the pile and the development of the limit unit shaft resistance. Special focus was placed on the operative value of the lateral earth pressure coefficient when the limit shaft resistance was reached. Figure 1 shows the influence of the initial vertical effective stress (σ'_v = 50, 100, 200 and 500 kPa) and of the relative density D_R of the sand on the K/K_0 ratio (for K_0 = 0.4, where K_0 is the coefficient of lateral earth pressure at rest).

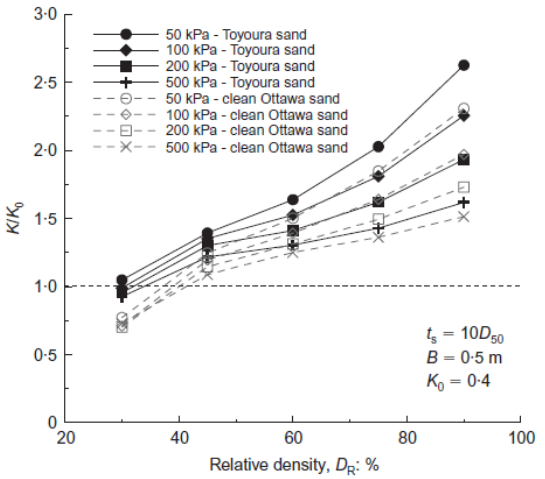

Figure 1. Effect of initial effective vertical stress and relative density on K/K_0 (Loukidis and Salgado 2008)

Figure 2 shows the influence of K_0 (K_0 = 0.4, 0.5, 1 and 2) and relative density on K/K_0 for Toyoura sand. In Figures 1 and 2, t_s is the thickness of the shear band at the pile-soil interface, while B is the diameter of the nondisplacement pile.

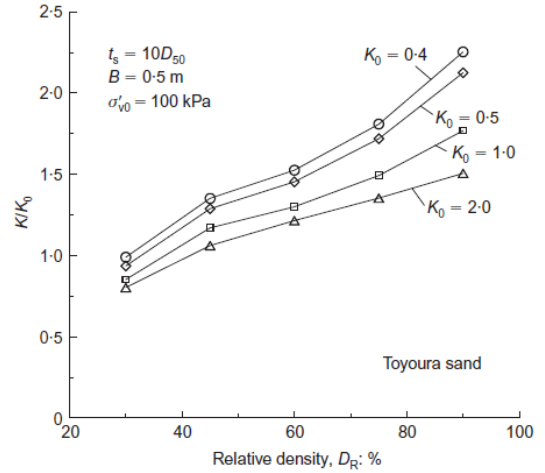

Figure 2. Effect of coefficient of lateral earth pressure at rest and relative density on K/K_0 for Toyoura sand (Loukidis and Salgado 2008)

According to Loukidis and Salgado (2008), K increases as the relative density of the sand increases and decreases as the initial vertical effective stress increases. Also, their results show that the K/K_0 ratio decreases as K_0 increases. Loukidis and Salgado (2008) proposed a relationship between the lateral earth pressure coefficient K and the initial relative density and stress state of the sand for use in the calculation of the limit unit shaft resistance of the pile:

$$K = \frac{K_0}{\exp(0.2\sqrt{K_0 - 0.4})} C_1 \exp\left(\frac{D_R}{100}\left[1.3 - 0.2\ln\left(\frac{\sigma'_v}{p_A}\right)\right]\right) \qquad [3]$$

where D_R is the relative density of the sand expressed as a percentage, and p_A is the reference stress (100 kPa). The above equation captures the dependence of K on the relative density of the sand and vertical effective stress (i.e. depth) and reliably predicts K for angular and rounded sands. Loukidis and Salgado (2008) found that the coefficient C_1 is equal to 0.71 for angular sands (based on results for Toyoura sand, which is angular) and is equal to 0.63 for rounded sands (based on results for Ottawa sand) and suggested a value of C_1 = 0.7 to be used in calculations for clean sands in general. Loukidis and Salgado (2008) also indicated that the angle δ is approximately equal to the triaxial-compression, critical-state friction angle ϕ_c. Thus, $\delta = \phi_c$ can be assumed in calculations without any significant error.

Loukidis and Salgado (2008) attempted an interpretation of centrifuge tests presented by Fioravante (2002) and Colombi (2005) by using finite element modelling and the soil-disk approach. In these tests, the diameter of the model piles was 10 mm, which represented a prototype pile in the field with a diameter of 0.8 m (applied centrifuge acceleration of 80g). For the case of Toyoura sand, the ratio of the model pile diameter B_m (= 10 mm) to D_{50} is approximately 53. Therefore, the size of the adjacent element to the prototype pile is set to 0.19B (= $10D_{50}B/B_m$). Figure 3 shows a comparison between the finite element analysis predictions of β with centrifuge test data (Fioravante 2002, Colombi 2005). It is clear that, when the shear band thickness is scaled up from the centrifuge tests correctly (t_s = 0.19B = 152 mm), the comparison is very favorable.

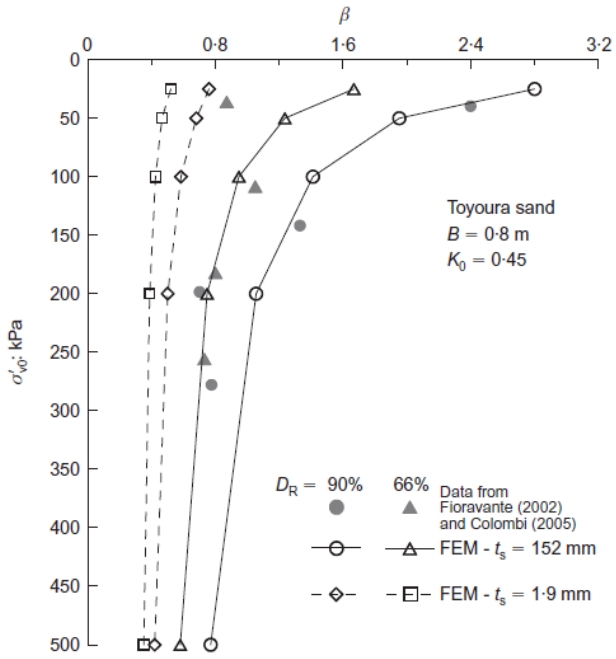

Figure 3. Effect of vertical effective stress on values of β from soil disc simulations with $t_s = 10D_{50}$ = 1.9 mm as well as t_s = 0.19B = 152 mm compared with centrifuge test data (from Loukidis and Salgado, 2008).

3.2 Unit Base Resistance

Determination of the unit base resistance is a key element in the design of piles bearing in sands since the shaft resistance is fully mobilized well before the maximum base resistance is reached. The ultimate unit base resistance $q_{b,ult}$ is a function of D_R, σ'_v and ϕ_c. Based on pile load tests, some researchers have expressed $q_{b,ult}$ as a fraction of the cone penetration resistance q_c (e.g., Ghionna et al. 1994) on the basis that the cone penetration test (CPT) can be viewed as a scaled-down pile load test, and q_c is approximately equal to the limit unit base resistance q_{bL} that a pile would have upon plunging. However, the $q_{b,ult}$ / q_{bL} (or $q_{b,ult}$ / q_c) values proposed by these researchers vary over a somewhat wide range (Salgado 2008). Lee and Salgado (1999) used nonlinear finite element analysis and calibration chamber plate load tests to find that $q_{b,ult}$ / q_{bL} depends primarily on D_R. Table 1 shows the effect of relative density on $q_{b,ult}$ / q_{bL} corresponding to the values of relative settlement s/B = 5% and 10%, where s is the pile settlement and B is the pile diameter, resulting from the finite element analyses and plate load tests. Table 1 suggests that, as the relative density increases, the normalized base resistance $q_{b,ult}/q_c$ decreases.

Table 1: Values of $q_{b,ult}/q_c$ at s/B =5% and s/B =10% (from Lee and Salgado 1999)

Pile Length (m)	D_R (%)	q_c (kPa)	$q_{b,ult}/q_c$ (s/B = 5%)	$q_{b,ult}/q_c$ (s/B = 10%)
5	30	7,157	0.13	0.21
	50	12,052	0.11	0.17
	70	19,562	0.09	0.14
	90	30,121	0.07	0.12
10	30	10,922	0.12	0.20
	50	17,544	0.10	0.17
	70	26,644	0.09	0.15
	90	38,816	0.08	0.13
20	30	16,716	0.12	0.19
	50	25,694	0.10	0.16
	70	36,718	0.09	0.15
	90	50,524	0.08	0.14

Lee and Salgado (1999) also show that at lower relative densities the effect of increasing the initial coefficient of lateral earth pressure K_0 on the normalized base resistance $q_{b,ult}/q_c$ is more significant (Figures 4).

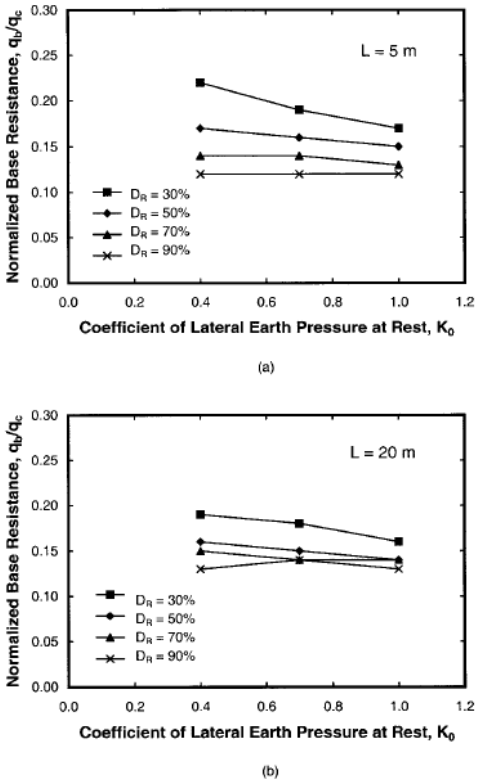

Figure 4. Effect of coefficient of lateral earth pressure at rest on normalized base resistance for different relative densities: a) pile length = 5m. b) pile length = 20m (Lee and Salgado 1999).

Based on the results of these analyses, Salgado (2008) proposed an equation for $q_{b,ult}$ corresponding to 10% relative settlement (i.e., the unit base resistance q_b corresponding to a pile head settlement of 10% of the pile diameter):

$$q_{b,ult} = q_{b,10\%} = 0.23\exp(-0.0066D_R)\,q_{bL} \quad [4]$$

To obtain $q_{bL} = q_c$, Salgado and Prezzi (2007) performed a rigorous cavity expansion analysis for sand in terms of fundamental soil variables (see Eq. 5). A simplified stress rotation analysis allowed computation of cone resistance from cavity limit pressure.

$$\frac{q_{bL}}{p_A} = 1.64\exp(0.1041\phi_c + (0.0264 - 0.0002\phi_c)D_R)\left(\frac{\sigma'_h}{p_A}\right)^{0.841-0.0047D_R} \quad [5]$$

where $\sigma'_h = K_0\sigma'_v$ is the *in situ* horizontal effective stress and K_0 is the coefficient of lateral earth pressure at rest.

For the calculations of q_{bL} and $q_{b,10\%}$, representative values of ϕ_c, D_R and σ'_h must be selected in the zone below the pile base within which the resistance to downward movement of the pile develops. At the limit condition (i.e., when the pile is about to plunge), a plastic zone forms immediately below the pile base. On the other hand, the zone of influence for the condition corresponding to 10% relative settlement is somewhat wider and deeper for sand because there has not been localization of strains due to plasticity. As far as the authors know, there has been no study that conclusively outlines the exact extent of the zones of influence below the pile base under working and limit conditions. Therefore, we considered it appropriate to use the values of ϕ_c, D_R and σ'_h corresponding to a depth of $B_b/2$ below the pile base (B_b = pile base diameter) for calculating q_{bL} and $q_{b,10\%}$. This is conservative even in the event that a large influence depth would be in effect, except of course if there is a weak layer within reach of the pile base.

Based on Eq. 5 Salgado and Prezzi (2007) also proposed a more reliable and practical method of calculating D_R from CPT results:

$$D_R(\%) = \frac{\ln\left(\frac{q_c}{p_A}\right) - 0.4947 - 0.1041\phi_c - 0.841ln\left(\frac{\sigma'_h}{p_A}\right)}{0.0264 - 0.0002\phi_c - 0.0047ln\left(\frac{\sigma'_h}{p_A}\right)} \quad [6]$$

Equations 3 to 6 for calculating shaft and base capacities were obtained from rigorous analyses that mechanistically relate the pile capacities to the fundamental soil. Additionally, results from these equations have been compared against specific, high-quality experimental data. These equations form the

basis for the Purdue Sand Method for Nondisplacement Piles (PSM-NP).

4 PURDUE CLAY METHOD FOR NONDISPLACEMENT PILES

Researchers at Purdue University have also developed design methods for the limit unit base and shaft resistances of nondisplacement piles in clay. This section is dedicated to reviewing the design equations developed by Chakraborty et al. (2011), Salgado et al. (2011) and Salgado et al. (2004).

4.1 Limit Unit Shaft Resistance

The α method is used widely to calculate the limit unit shaft resistance q_{sL} in clay:

$$q_{sL} = \alpha s_u \quad [7]$$

where s_u is the undrained shear strength of clay and α is the undrained shaft resistance coefficient. Calculations of the shaft resistance of drilled shafts installed in clay are most often performed using empirical correlations (e.g., Skempton 1959, O'Neill and Reese 1999) developed based on a limited number of pile load tests. To determine α in a more scientific way, finite element analyses were performed with an advanced two-surface-plasticity constitutive model for clay. The clay constitutive model (see Basu et al. 2010) reproduces the mechanical response of clays under multi-axial loading conditions and predicts both drained and undrained behavior of clay at small and large strains. It is also able to capture the drop in strength towards a residual value at very large shear strains. One-dimensional axisymmetric finite element analyses were performed in order to simulate the essential stages of the installation and loading of drilled shafts in clay; the analyses considered different initial stresses, different overconsolidation ratios, and different values for the difference between the critical-state and the minimum residual friction angles. Based on the analyses performed using properties of London Clay (LC) and San Francisco Bay Mud (SFBM), the following equation was proposed for α:

$$\alpha = \left(\frac{s_u}{\sigma'_v}\right)^{-0.05} \left[A_1 + (1 - A_1) exp\left\{-\left(\frac{\sigma'_v}{p_A}\right)\left(\phi_c - \phi_{r,min}\right)^{A_2}\right\}\right] \quad [8]$$

where σ'_v is the *in situ* vertical effective stress at the depth at which q_{sL} is calculated, ϕ_c is the critical-state friction angle, $\phi_{r,min}$ is the minimum residual state friction angle, and p_A is the reference stress value (100*k*Pa). The value of A_1 is obtained from:

$$A_1 = \begin{cases} 0.4 & \phi_c - \phi_{r,min} \geq 12° \\ 0.75 & \phi_c - \phi_{r,min} \leq 5° \end{cases} \quad [9]$$

A_1 is linearly interpolated for $5° \leq \phi_c - \phi_{r,min} \leq 12°$. A_2 is a coefficient determined as:

$$A_2 = 0.4 + 0.3ln\left(\frac{s_u}{\sigma'_v}\right) \quad [10]$$

The above equations capture the dependence of the unit shaft resistance on the clay undrained shear strength, the normal effective stress and the difference between the critical-state friction angle and the minimum residual-state friction angle. Figures 5 through 7 provide the values of α for London clay long after pile installation that resulted from the finite element analyses and Eqs. 8-10.

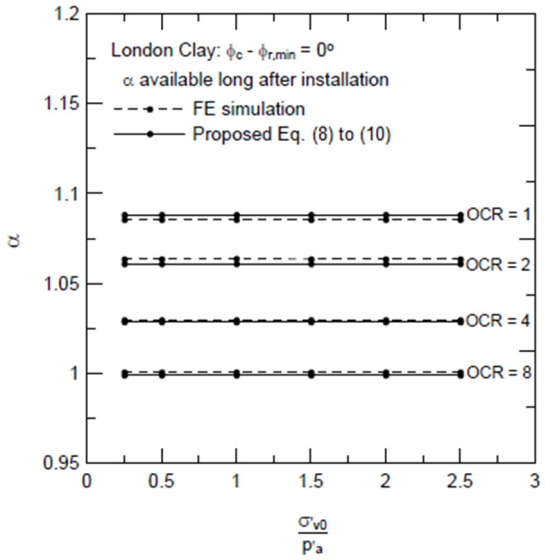

Figure 5. α values from FE analysis and Eqs. 8-10 for $\phi_c - \phi_{r,min} = 0$ degree (from Chakraborty et al. 2011)

Figures 5 to 7 clearly show that the values of α decrease with increasing OCR, increasing σ'_{v0} and decreasing residual-state friction angle. Figure 8 shows normalized unit shaft resistance q_{sL}/σ'_{v0} versus normalized undrained shear strength s_u/σ'_{v0}. Since the proposed relations have the key intrinsic variables of the clay as parameters, they are of general applicability. To illustrate an application of the correlations, calculated values for $\phi_c - \phi_{r,min} = 0$ and for $\phi_c - \phi_{r,min} = 10$ are compared with load test data from Bryan, Texas load test site (Engeling and Reese 1974). Since no information on $\phi_{r,min}$ of the Bryan clay was available, we use a range of $\phi_c - \phi_{r,min}$ between 0 and 10; it is clear that the test data fall well within this range.

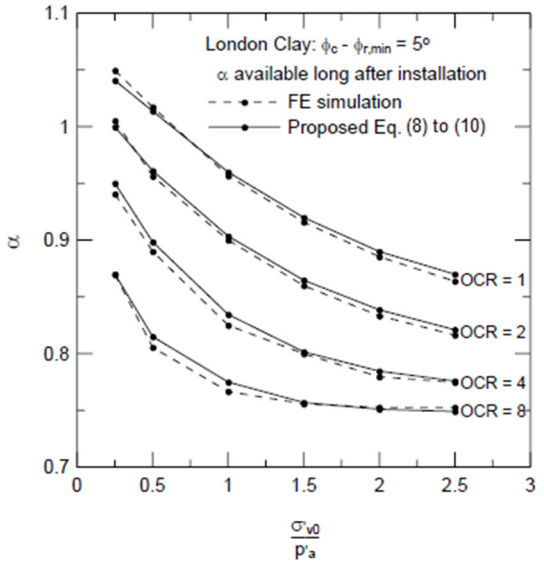

Figure 6. α values from FE analysis and Eqs. 8-10 for $\phi_c - \phi_{r,min} = 5$ degrees (from Chakraborty et al. 2011)

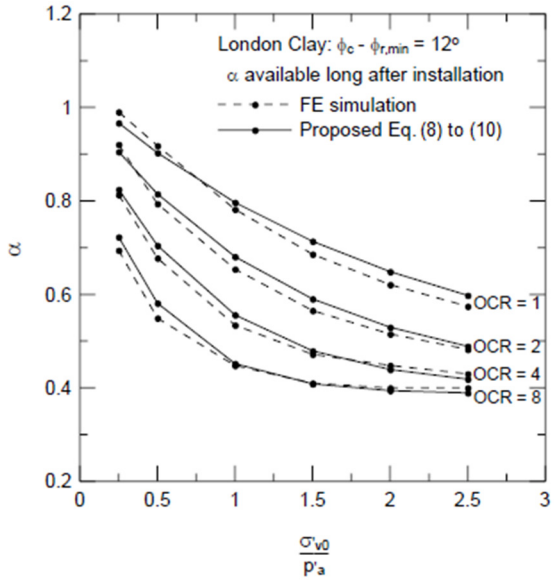

Figure 7. α values from FE analysis and Eqs. 8-10 for $\phi_c - \phi_{r,min} = 12$ degrees (from Chakraborty et al. 2011)

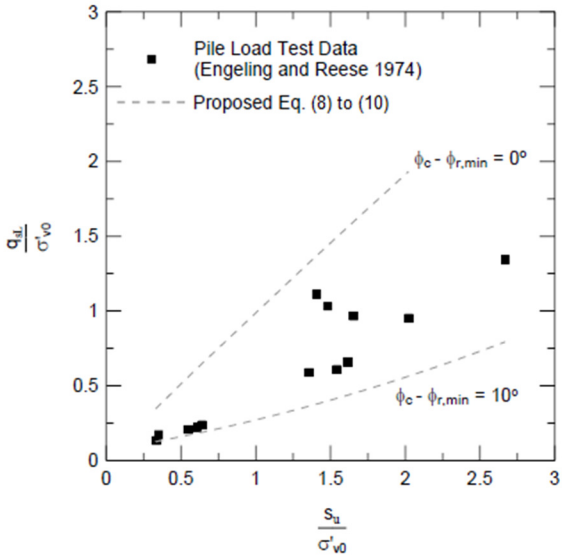

Figure 8. Comparison of normalized unit shaft resistance with load test data from Bryan, Texas load test site (Engeling and Reese 1974) (from Chakraborty et al. 2011)

4.2 Unit Base Resistance

Geotechnical engineers routinely use the bearing capacity equation to estimate the limit unit load q_{bL} that causes a footing to undergo classical bearing capacity failure. The bearing capacity equation for circular piles embedded in clay has the following form:

$$q_{bL} = q_{bL}^{net} + q_0 = N_c\, s_u + q_0 \qquad [11]$$

where q_{bL}^{net} is the net unit bearing capacity, q_0 is the surcharge at the pile base level, and q_{bL} is the limit unit base resistance at the pile base, $N_c = q_{bL}^{net}/s_u$ is the bearing capacity factor that has traditionally been within the 9-11 range for clays, and s_u is the undrained shear strength at the pile base.

Salgado et al. (2004) used finite element limit analysis of circular foundations in perfectly-plastic Tresca soil with an associated flow rule to obtain lower and upper bounds on N_c. Based on these analyses, Salgado et al. (2004) found that the lower and upper bound values of N_c increases with increasing relative depth D/B (the ratio of the length of the pile to the diameter of the pile), as shown in Figure 9.

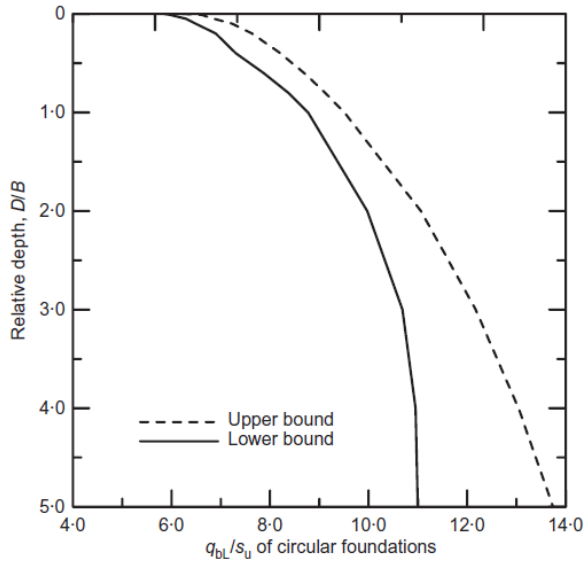

Figure 9. Limit unit base resistance of circular foundation versus depth (Salgado et al. 2004)

For D/B = 5, the lower and upper bound values of N_c are equal to 11.0 and 13.7, respectively. Salgado et al. (2004) indicate that it is possible that $N_c = q_{bL}^{net}/s_u$ would continue to increase with increasing D/B beyond D/B = 5, as the flattening of the curve from D/B = 4 to D/B = 5 may be due to a mesh that is not sufficiently fine for such deep elements. These results suggest that the current practice in pile base capacity estimation may be as much as 20–30% over-conservative. However, Salgado et al. (2004) stressed that limit analysis may miss aspects of the interaction between foundation base and soil for deep foundations, which seems to be approximated by a cavity expansion process. They also mentioned that assumptions made regarding the material (perfect plasticity and associated flow) may also have a more significant impact on the calculation of the end bearing of a deep foundation, which develops under more constrained conditions than those of a shallow foundation.

Equations 8 through 11 constitute the basis for the Purdue Clay Method for Nondisplacement Piles (PCM-NP).

5 SUMMARY AND CONCLUSIONS

In this paper, we reviewed the soil property-based design equations for nondisplacement piles in sand and clay that were developed over the last decade at Purdue University. Rigorous analyses combined with advanced constitutive models were used to develop the Purdue Sand and Clay Methods for Nondisplacement Piles.

Finite element analysis coupled with an advanced constitutive model was used to propose a relationship between the lateral earth pressure coefficient K and the initial density and stress state of the sand. Based on the results of the numerical analysis, it was found that K increases as the relative density increases, while it decreases with increases in the initial vertical effective stress. Also, the ratio of K/K_0 decreases as K_0 increases. It was also established that the interface friction angle between the pile and soil δ is approximately equal to the triaxial-compression critical-state friction angle ϕ_c.

The base resistance of a nondisplacement pile in sand was analyzed using cavity expansion analysis and finite element analysis. It was found that as the relative density increases, the normalized base resistance $q_{b,ult} / q_c$ decreases. At lower relative densities, the effect of the initial coefficient of lateral earth pressure at rest K_0 on the normalized base resistance $q_{b,ult} / q_c$ is more significant

Finite element analysis coupled with an advanced constitutive model was used to develop design equations for the shaft resistance of nondisplacement piles in clay. The α values decrease with increasing OCR, increasing σ'_{v0} and decreasing residual-state friction angle.

The base capacity of circular piles in clay was investigated using finite element limit analysis For D/B = 5, the lower and upper bound values of N_c are equal to 11.0 and 13.7, respectively.

6 REFERENCES

Basu, P., Salgado, R., Prezzi, M. And Chakraborty, T. 2009. A method for accounting for pile set up and relaxation in pile design and quality assurance. Joint Transportation Research Program, SPR-2930.

Chakraborty, T., Salgado, R., Basu, P., and Prezzi, M. 2011 The shaft resistance of drilled shafts in clay. Working paper.

Colombi, A. 2005. Physical Modelling of an Isolated Pile in Coarse Grained Soils. Ph.D. Thesis, Univ. of Ferrara.

Engeling, D. and L. C. Resse 1974, Behavior of Three Instrumented Drilled Shafts under Short Term Axial Loading. Proyect 3-5-72-176, conducted for the Texas Highway Department.

Fioravante, V. 2002. On the shaft friction modelling of non-displacement piles in sand. *Soils and Foundations*. 42(2), 23-33.

Ghionna, V. N., Jamiolkowski, M., Pedroni, D. And Salgado, R. 1994. The tip resistance of drilled shafts in sands. Vertical and Horizontal Deformations of Foundations and Embankments, *Proc. Settlement '94 ASCE 2*, 1039-1057.

Lee, J. H. and Salgado, R. 1999. Determination of pile base resistance in sands. *Journal of Geotechnical and Geoenvironmental Engineering*, 125(8), 673-683.

Loukidis, D., Salgado, R. and Abou-Jaoude, G. 2008. Assessment of Axially-Loaded Pile Dynamic Design Methods and Review of INDOT Axially-Loaded Pile Design Procedure. FHWA/IN/JTRP-2008/6, Purdue Univ.

Loukidis, D. and Salgado, R. 2008. Analysis of shaft resistance of non-displacement piles in sand. *Géotechnique* 58(4), 283-296.

Loukidis, D. and Salgado, R. 2009. Modeling sand response using two-surface plasticity. *Computers and Geotechnics* 36(1-2), 166-186.

O'Neill, M. W. and Hassan, K. M. 1994. Drilled shafts: effects of construction on performance and design criteria. *Proc. Int. Conf. Design Constr. Deep Fdns*, Orlando, Florida. 137-187.

O'Neill, M. W. and Reese, L. C. 1970, Behavior of axially loaded drilled shafts in Beaumont clay. Research Report No. 89-8, Center for Highway Research.

O'Neill, M. W. and Reese, L. C. 1999. Drilled shafts: Construction procedures and design methods. Report No. FHWA-IF-99-025, FHWA.

Reese, L. C., Touma, F. J. and O'Neill, M. W. 1976. Behavior of drilled piers under axial loading. *Journal of Geotechnical. Engineering Division*, 102(5), 493-510.

Salgado, R. 2008. *The Engineering of Foundations*. McGraw Hill, USA.

Salgado, R. and Prezzi, M. 2007. Computation of cavity expansion pressure and penetration resistance in sands." *International Journal of Geomechanics*. 7(4), 251-265.

Salgado, R., Woo, S.I., and Kim, D.W. 2011. *Development of Load and Resistance Factor Design for Ultimate and Serviceability Limit States of Transportation Structure Foundations, Research Report No. 3108, JTRP.*

Salgado, R., Lyamin, A. V., Sloan, S. W., and Yu, H. S. 2004. Two- and three-dimensional bearing capacity of foundations in clay. *Géotechnique*, 54(5), 297-306.

Skempton, A. W. 1959. Cast in situ bored piles in London clay. Geotechnique, 9(4), 153–173.

Stas, C. V. and Kulhawy, F. H. 1984. Critical evaluation of design methods for foundations under axial uplift and compression loading. EPRI Report EL-3771, Research Project 1493-1, Electric Power Research Institute, Palo Alto, California.